

Injection of ethanol into supercritical CO₂: Determination of mole fraction and phase state using linear Raman scattering

Andreas Braeuer^{1*}, Stefan Dowy¹, and Alfred Leipertz¹,
Robert Schatz² and Eberhard Schluecker²

¹Lehrstuhl für Technische Thermodynamik, Universität Erlangen-Nürnberg, Am Weichselgarten 8, 91058
Erlangen, Germany

²Lehrstuhl für Prozessmaschinen und Anlagentechnik, Universität Erlangen-Nürnberg, Cauerstrasse 4, 91058
Erlangen, Germany
ab@ltt.uni-erlangen.de

Abstract: For the pulsed injection of liquid ethanol into supercritical CO₂ inside an optically accessible chamber, for the first time to the best of our knowledge the spatially and temporally resolving linear Raman scattering technique was used to simultaneously determine the mole fraction and the corresponding phase state in the ethanol jet. The mole fraction was identified by calculating the ratio of the C-H band Raman signal (2950 cm⁻¹) of ethanol and the CO₂ Raman signal. The magnitude of this ratio was found to be phase state sensitive. Thus, the phase state of the mixture of ethanol and CO₂ could be classified as being homogeneous liquid, homogeneous supercritical or not yet homogeneously mixed.

©2007 Optical Society of America

OCIS codes: (170.0170) Medical optics and biotechnology; (290.5860) Scattering, Raman; (300.6450) Spectroscopy, Raman; (999.9999) Advanced fluids diagnostics

References and links

1. J. Joung and M. Perrut, "Particle design using supercritical fluids: Literature and patent survey," *J. Supercrit. Fluids* **20**, 179-219 (2001).
2. Z. Knez and E. Weidner, "Particles formation and particle design using supercritical fluids," *Curr. Opin. Solid State Mater. Sci.* **7**, 353-361 (2003).
3. E. Reverchon and R. Adami, "Nanomaterials and Supercritical Fluids," *J. Supercrit. Fluids* **37**, 1-22 (2006).
4. E. Reverchon, G. Caputo, and I. De Marco, "Role of phase behavior and atomization in the supercritical antisolvent precipitation," *Ind. Eng. Chem. Res.* **42**, 6406-6414 (2003).
5. K. Suzuki and H. Sue, "Isothermal vapor liquid equilibrium data for binary systems at high pressures: Carbon dioxide-methanol, carbon dioxide-ethanol, carbon dioxide-1-propanol, methane-ethanol, methane-1-propanol, ethane-ethanol, and ethane-1-propanol systems," *J. Chem. Eng. Data* **35**, 63-66 (1990).
6. C. Day, C. J. Chang, and C-Y. Chen, "Phase equilibrium of ethanol + CO₂ and acetone + CO₂ at elevated pressures," *J. Chem. Eng. Data* **41**, 839-843 (1996).
7. B. E. Poling et al., *The properties of gases and liquids* (McGraw-Hill, 2001)
8. A. Braeuer, F. Beyrau, M. C. Weikl, T. Seeger, J. Kiefer, A. Leipertz, A. Holzwarth, A. Soika, "Investigation of the combustion process in an auxiliary heating system using dual-pump CARS," *J. Raman Spectrosc.* **37**, 633-640 (2006).
9. A. Braeuer, R. Schatz, E. Schluecker, A. Leipertz, "Characterisation of the spray dynamics in the pulsed anisolvant spray precipitator," in proceedings of ICLASS (Kyoto, Japan, 2006) paper ID ICLASS06-274.
10. G. Herzberg, *Molecular spectra and molecular structure*, (Van Nostrand Company, New York 1966).
11. M. Lapp and C. M. Penney, eds., *Laser Raman Gas Diagnostics*, (Plenum Press, New York 1974).
12. A. C. Eckbreth, *Laser diagnostics for combustion temperature and species* (Gordon and Breach, Amsterdam 1996).
13. K. Kohse-Höinghaus and J. B. Jeffries, *Applied combustion diagnostics*, (Taylor and Francis, New York 2002).
14. T. Müller, G. Grünefeld, V. Beushausen, "High-precision measurement of the temperature of methanol and ethanol droplets using spontaneous Raman scattering," *Appl. Phys. B.* **70**, 155-158 (2000).
15. P. C. Miles, "Raman line imaging for spatially and temporally resolved mole fraction measurements in internal combustion engines," *Appl. Opt.* **38**, 1714-1732 (1999).

16. M. Taschek, J. Egermann, S. Schwarz, and A. Leipertz, "Quantitative analysis of the near-wall mixture formation process in a passenger car direct-injection Diesel engine by using linear Raman spectroscopy," *Appl. Opt.* **44**, 6606-6615 (2005).
17. M. C. Weigl, F. Beyrau, J. Kiefer, T. Seeger, and A. Leipertz, "Combined coherent anti-Stokes Raman spectroscopy and linear Raman spectroscopy for simultaneous temperature and multiple species measurements," *Opt. Lett.* **31**, 1908-1910 (2006).
18. A. Stratmann and G. Schweiger, "Fluid phase equilibria of ethanol and carbon dioxide mixtures with concentration measurements by Raman spectroscopy," *Appl. Spectrosc.* **56**, 783-788 (2002).
19. H. W. Schrötter and H. W. Klöckner, *Raman spectroscopy of gases and liquids*, (Springer, 1979).

1. Introduction

The provision of fine and uniform particles is essential for the development of products with new and improved characteristics, enabling a targeted drug delivery but also in the field of other pharmaceutical, medical or biological applications. Also, if heat and impact sensitive materials are produced, special requirements during the particle generation process have to be regarded [1]. To meet these demands, one well reputed method can be found in supercritical high pressure precipitation processes. In the supercritical antisolvent process (SAS) a dilution consisting of a solute (A) and a solvent (S) is injected into a supercritical antisolvent (AS). Because of the unlimited solubility of S in AS and vice versa and the high diffusion potential of supercritical fluids, there is a rapid mixture of all three components A, S, and AS. As the solubility of A in AS is negligible small, the supersaturation of A is compensated by the rapid start of particle precipitation. The potentials of the SAS process are reviewed by Knez and Weidner in 2003 [2] and by Reverchon and Adami in 2006 [3].

Reverchon et al. [4] proved, that the characteristics of the resulting particle size distribution and its morphology can be manipulated by adjusting the operation conditions of the SAS process to certain regimes in the p - x phase diagram of solvent and antisolvent as given in Fig. 1 for the ethanol/ CO_2 system at 313 K.

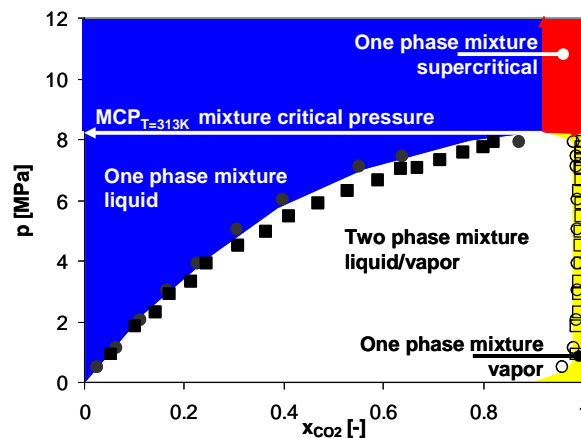


Fig. 1. p - x phase diagram of a binary ethanol/ CO_2 system for 313 K. Discs from Suzuki et Saito [5], squares from Day et al. [6].

Here, x_{CO_2} represents the mole fraction of CO_2 and is defined as (n is number of moles)

$$x_{\text{CO}_2} = n_{\text{CO}_2} / (n_{\text{CO}_2} + n_{\text{EtOH}}). \quad (1)$$

According to Gibbs law, at isothermal conditions the mixture phase state is only governed by the pressure and by the mixture mole fraction. Below the mixture critical pressure (MCP) a mixture of ethanol (EtOH) and CO_2 can exist in the liquid phase, in the vapor phase, or in the two phase region where the liquid and the vapor phase are coexistent. If for a certain pressure below the MCP the overall mole fraction is within the two phase region, the solid symbols in

Fig. 1 give the mole fraction of the liquid phase, whereas the open symbols in Fig. 1 give the mole fraction of the coexistent vapor phase [5, 6]. Above the MCP, there is only one phase existent which is either liquid or supercritical. As phase diagrams hold for thermodynamic equilibrium conditions only, the exact mixing conditions during the highly turbulent mixing process of the injected liquid solvent and the supercritical antisolvent cannot be extracted from this strategy.

We introduce the application of the linear Raman scattering technique to detect the mole fraction and the corresponding phase state during the highly turbulent mixing process at non equilibrium conditions with a high temporal resolution of a few nanoseconds. As this communication focuses on the capability of the linear Raman scattering technique to analyze the process of mixture formation for supercritical precipitation processes, only pure ethanol injection (pure solvent without solute) into supercritical CO₂ is considered. The critical point of CO₂ is defined by a temperature of 304.12 K and a pressure of 7.374 MPa [7].

2. Experimental setup

The experimental setup of the Raman sensor is illustrated in Fig. 2.

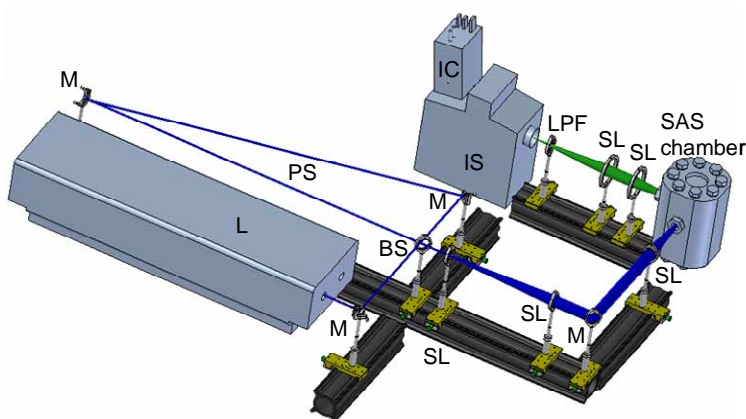


Fig. 2. Experimental Raman setup; L: Nd:YAG-laser, SL: spherical lens, M: mirror, BS: beam splitter, IS: imaging spectrophotometer, IC: ICCD camera, LPF: long pass filter

For the excitation of the Raman transitions a pulsed frequency tripled Nd:YAG-laser at 355 nm with a maximum single-pulse energy of 250 mJ and a pulse length of 10 ns (FWHM) was used. 200 mJ pulse energy could be irradiated through the sapphire windows of the optically accessible chamber, without exceeding the window damage threshold [8] because of two arrangements. First, the laser pulse was expanded in time by a single loop pulse stretcher to decrease the single shot energy flux. Second, the laser beam was expanded from its original diameter of 9 mm to 45 mm by using a telescope ($f_1 = -100$ mm, $f_2 = 500$ mm) to decrease the energy density inside the sapphire windows. Then, the laser beam was focused in the middle of the chamber downstream the injector's nozzle exit by a $f = 300$ mm lens. The distance between the two sapphire windows was 60 mm. The probe volume (beam waist along the focus of the laser beam) was imaged with a magnification of 1.5 via two convex lenses onto the slit (300 μ m) of an imaging spectrometer. An intensified CCD-camera at the exit of the spectrometer allowed the locally resolved acquisition of the Raman spectra. The detector pixels of the camera were binned 8 times 2 to form superpixels. This resulted in 48 superpixel rows (spatial axis), each of 288 superpixels in length (spectral axis). Thus, one line of 7 mm in length is spatially resolved by only one single laser-shot in increments of 140 μ m.

A detailed description of the SAS chamber is given elsewhere [9]. The injection duration and the injection frequency of the piezoelectric actuated injector were constantly set at 1.5 ms and 1 Hz, respectively. The injector's nozzle is identical to a standard diesel injector nozzle

but has only one capillary at the tip with a diameter of 100 μm and a length of 0.2 mm. The solvent used for the calibration and the injection experiments was denatured EtOH (1 Vol % petrol ether).

3. Calibration of the Raman setup for mixture analysis

Upon irradiation of laser light into a sample of molecules an interaction between the photons and the molecules takes place in form of light scattering which can be elastic, with no frequency shift between the incident and the scattered light (Rayleigh scattering), but also inelastic with a molecule specific frequency shift between the incident laser frequency and the scattered frequency (Raman scattering) (see e.g. Ref. [10]). Raman scattering can be used for fluid temperature and gas species concentration measurements [11-13] covering a broad field of applications (see e.g. for combustion diagnostics Refs. [14-17]). In the field of particle and process technology which is the main focus of application here, only few investigations have been done [18]. As nearly all molecules are Raman active [10], from the Raman spectrum a simultaneous detection of different species is possible. Fig. 3(a) shows the Raman spectra of an EtOH/ CO_2 mixture for the liquid and the supercritical state for a mole fraction of $x_{\text{CO}_2} = 0.68$.

In Fig. 3(a) both spectra are normalized to the C-H Raman signal peak of EtOH at a Raman shift of around 2950 cm^{-1} . Between 500 and 1500 cm^{-1} it can clearly be seen that at supercritical conditions the C-C and the C-H Raman signals of EtOH are overwhelmed by the CO_2 Raman signal (two peaks at 1388 and 1286 cm^{-1}), whereas for liquid conditions for the same mole fraction the EtOH C-H and C-C Raman signals can be detected simultaneously with the CO_2 Raman signal peaks. Similar behavior is known for hydrocarbons for a phase change from liquid to gas [19]. The phase sensitive Raman scattering cross section for liquid hydrocarbons is reported to be up to five times larger than for gaseous hydrocarbons. In Fig. 3(a) another phase state sensitive spectrum change can be identified which is related to the spectral shape of the O-H Raman signal of EtOH. For liquid EtOH/ CO_2 mixtures the O-H Raman signal of EtOH is broad while for supercritical conditions it is narrower with its maximum at a different spectral position. This effect can be related to the density changes which affect the interaction of hydrogen bonding and was previously used by Müller et al. [14] to determine droplet temperatures in vaporizing sprays.

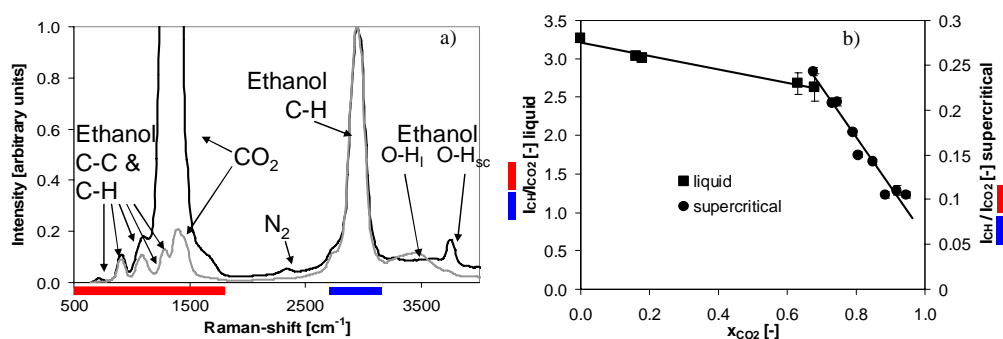


Fig. 3. (a). Raman spectra of a homogeneous EtOH/ CO_2 mixture with a mole fraction of $x_{\text{CO}_2} = 0.68$ at two different temperatures above the MCP; supercritical (black line) and liquid (gray line) (b). Mole fraction calibration of the peak intensity ratio of the C-H Raman signal around 2950 cm^{-1} to the CO_2 Raman signal for homogeneous liquid mixtures (squares) and supercritical mixtures (discs)

In Fig. 3(a) two spectral regions are highlighted in red and blue. The blue region indicates the spectral region which was evaluated to determine the C-H Raman signal intensity of EtOH. The red region marks the spectral region which was evaluated to determine the CO_2 Raman signal intensity. In the red region, especially for liquid mixtures, the C-C and the C-H Raman signals of EtOH give a strong signal interference to the CO_2 Raman signal intensity.

Having calibrated the signal intensity ratio I_{CH}/I_{CO_2} of the blue (C-H Raman signal of EtOH) and the red spectral region (CO_2 Raman signal) for different mole fractions as shown in Fig. 3(b), one can use this calibration data to determine the mole fraction distribution along the probe volume during the injection experiment. By considering the signal ratios only, fluctuations of the laser energy do not have an impact on the measured results in the linear Raman scattering regime. Nevertheless, the error bars in Fig. 3(b) indicate the standard deviation of 50 single-shot measurements. For supercritical conditions the error bars cannot be seen, as they are smaller than the data points (discs) themselves. The calibration was conducted with the same experimental setup which was used for the injection experiments. To guarantee homogeneous one phase mixture conditions during calibration the MCP had to be exceeded. By increasing the temperature the supercritical area of EtOH/ CO_2 mixtures shifts to higher MCP and smaller mole fractions than given for 313 K in Fig. 1 [5, 6]. Hence we were able to create a mole fraction overlap for the liquid state and the supercritical state calibration curves which were both assumed as straight lines. For mole fractions $x_{CO_2} > 0.98$ the calibration line may not be extrapolated, as the slope of the calibration data decreases to intersect at $I_{CH}/I_{CO_2} = 0$ and $x_{CO_2} = 1$. Thus, for the investigated experimental conditions of the injection process, signal intensity ratios that correspond to mole fractions $x_{CO_2} > 0.98$ were evaluated as supercritical and set to $x_{CO_2} = 1$. For not homogeneously mixed state conditions during the injection experiments on a scale which is smaller than the spatial resolution of the detection system, intensity ratios I_{CH}/I_{CO_2} between 0.24 and 2.63 will result, for which no calibration data is available, see Fig. 3(b). Hence, according to the state sensitive Raman scattering cross section of EtOH an evaluation of the mole fraction in this regime is not possible. In this case the mole fraction was set to $x_{CO_2} = 0.5$ and the mixture state was assumed to be both, liquid and supercritical.

4. Results

During the injection experiments EtOH was injected with 35 MPa into the injection chamber which was pressurized with CO_2 to 12.5 MPa at 313 K. Fig. 4 represents the evaluated mole fractions and the corresponding state 5 mm and 7 mm downstream the injector's nozzle 0.5 ms after visible start of injection (see injection image in Fig. 4).

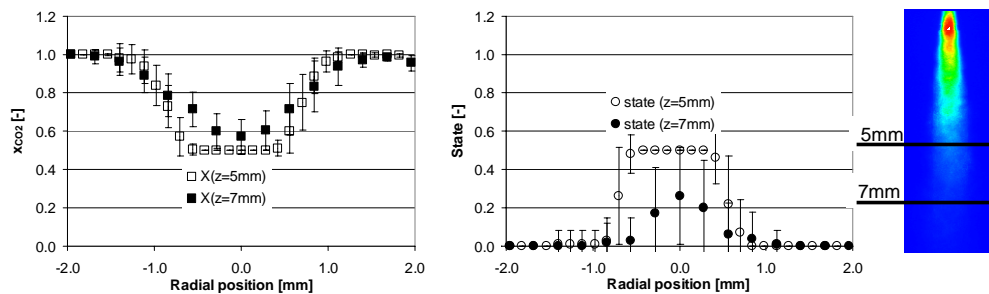


Fig. 4. Mole fraction and corresponding phase state in dependence on the radial position 5 mm and 7 mm downstream the nozzle exit for an injection pressure of 35 MPa and a chamber pressure of 12.5 MPa at 313 K. A spray image by elastic light scattering is inserted into the figure for orientation.

One single laser shot allowed to resolve 7 mm radial position inside the chamber in steps of 0.280 mm (binning = 16x2) and 0.140 mm (binning = 8x2) for 7 mm and 5 mm downstream the injector, respectively. In Fig. 4 only radial positions of the results within 4 mm are presented. The centre of the radial position indicates the position of the nozzle in the chamber. The presented data are mean values of 50 single-shot measurements. The given error bars indicate the corresponding standard deviation, which are shot-to-shot fluctuations of the pulsed injection process. The mole fraction results are given in absolute numbers. For the phase state of the mixture only values of 0 (supercritical mixture), 1 (liquid mixture) and 0.5

(supercritical and liquid state coexistent in a scale smaller than the spatial resolution of the detection system) are given. The interim state values of the mixture result from the averaging of 50 single-shots.

In contrast to the measurement position at $z = 7$ mm the measurement position at $z = 5$ mm shows no standard deviation for radial positions between -0.5 mm and $+0.5$ mm for both, the mole fraction and the phase state. This indicates that for these operation conditions every 50 single-shot measurements could not be evaluated with the calibration data presented in Fig. 3(b), as the intensity ratio $I_{\text{CH}}/I_{\text{CO}_2}$ was between 0.3 and 2.6. Thus, each of the 50 single-shot measurements were set to a mole fraction of 0.5 and a phase state of 0.5. At the border area of the EtOH jet between -2 mm and -1 mm and between 1 mm and 2 mm radial position the mean mole fractions take values larger than 0.5 and the mean phase state takes values smaller than 0.5. At measurement positions for which the phase state value is small or 0, the mole fraction of the most or all 50 single-shot measurements was evaluated from the supercritical calibration line. Then the standard deviation of the mole fraction dominantly results from the shot-to-shot mole fraction fluctuation in a homogeneous supercritical mixture. If the mean state value increases, an increasing amount of the 50 single-shot measurements was not evaluated with the supercritical calibration line, as the intensity ratios $I_{\text{CH}}/I_{\text{CO}_2}$ were larger than 0.3. Then, the standard deviation of the mole fraction is increasingly dominated by shot-to-shot fluctuations of the occurrence of homogeneous liquid mixtures, homogeneous supercritical mixtures or inhomogeneous mixtures where supercritical and liquid mixture states are existent on a scale smaller than the spatial resolution of the detection system. Of all results given in Fig. 4, no single measurement was evaluated to be of liquid state. Summarizing the results, it can be emphasized that the mixture is more homogeneous the further the spray has penetrated into the chamber. This can be seen at the center of the radial position because of the smaller state values, its larger standard deviation, the larger mole fractions, and their larger standard deviation.

5. Conclusion

In this work the one-dimensional linear Raman scattering technique was used to identify different mixing regimes during the injection of liquid EtOH into supercritical CO_2 . In addition to the mole fraction we were able to simultaneously determine locally resolved the phase state of the mixture. In the future the application of this measurement technique allows the detailed investigation of supercritical antisolvent processes, which constitute a consistent expanding field for fine and uniform particle generation in chemical engineering. The effects of temperature, pressure and chemical composition of the solvent must no longer be considered in a global approach via the p - x diagrams, but can be determined temporally and spatially resolved. As the information of the phase state of the mixture can be evaluated from the signal ratio $I_{\text{CH}}/I_{\text{CO}_2}$ without regarding the shape of the O-H Raman signal even two-dimensional measurements of the mole fraction and the corresponding phase state are possible using the linear Raman scattering technique. Characteristic time scales of mixing can be measured under real process conditions and will for the first time provide experimental data for modelling the particle precipitation process in supercritical antisolvent technologies.

Acknowledgment

The authors gratefully acknowledge the financial support of parts of the work by the German National Science Foundation (DFG).